# P$^+$ State of Nitrogenase P-Cluster Exhibits Electronic Structure of a [Fe$_4$S$_4$]$^+$ Cluster

Kresimir Rupnik,[†] Yilin Hu,[§] Chi Chung Lee,[§] Jared A. Wiig,[§] Markus W. Ribbe,*[,§] and Brian J. Hales*[,†]

[†]Department of Chemistry, Louisiana State University, Baton Rouge, Louisiana 70803, United States
[§]Department of Molecular Biology and Biochemistry, University of California, Irvine, California 92697, United States

ABSTRACT: Mo nitrogenase consists of two component proteins: the Fe protein, which contains a [Fe$_4$S$_4$] cluster, and the MoFe protein, which contains two different classes of metal cluster: P-cluster ([Fe$_8$S$_7$]) and FeMoco ([MoFe$_7$S$_9$C·homocitrate]). The P-cluster is believed to mediate the electron transfer between the Fe protein and the MoFe protein via interconversions between its various oxidation states, such as the all-ferrous state (P^N) and the one- (P$^+$) and two-electron (P^{2+}) oxidized states. While the structural and electronic properties of P^N and P^{2+} states have been well characterized, little is known about the electronic structure of the P$^+$ state. Here, a mutant strain of *Azotobacter vinelandii* (DJ1193) was used to facilitate the characterization of the P$^+$ state of P-cluster. This strain expresses a MoFe protein variant (designated Δ*nifB* β-188^{Cys} MoFe protein) that accumulates the P$^+$ form of P-cluster in the resting state. Magnetic circular dichroism (MCD) spectrum of the P-cluster in the oxidized Δ*nifB* β-188^{Cys} MoFe protein closely resembles that of the P^{2+} state in the oxidized wild-type MoFe protein, except for the absence of a major charge-transfer band centered at 823 nm. Moreover, magnetization curves of Δ*nifB* β-188^{Cys} and wild-type MoFe proteins suggest that the P^{2+} species in both proteins have the same spin state. MCD spectrum of the P$^+$ state in the Δ*nifB* β-188^{Cys} MoFe protein, on the other hand, is associated with a classic [Fe$_4$S$_4$]$^+$ cluster, suggesting that the P-cluster could be viewed as two coupled 4Fe clusters and that it could donate either one or two electrons to FeMoco by using one or both of its 4Fe halves. Such a mode of action of P-cluster could provide energetic and kinetic advantages to nitrogenase in the complex mechanism of N$_2$ reduction.
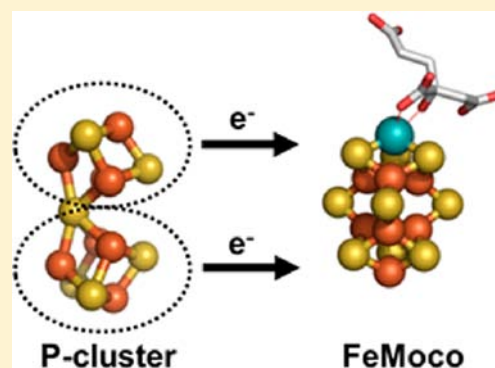
1. INTRODUCTION

Nitrogenase catalyzes the reduction of dinitrogen to ammonia. Mo nitrogenase, the most common form of this enzyme, consists of two protein components: the Fe protein and the MoFe protein. Both proteins are required for the enzymatic activity of nitrogenase, where the Fe protein serves as the obligate reductant of the MoFe protein.[1] The Fe protein has a γ_2 structure, and it contains a subunit-bridging [Fe$_4$S$_4$] cluster and one MgATP binding site in each subunit. The MoFe protein has an $\alpha_2\beta_2$ structure, and it contains two metal clusters in each $\alpha\beta$-dimer: the P-cluster ([Fe$_8$S$_7$]) and the FeMo cofactor (or FeMoco, [MoFe$_7$S$_9$C·homocitrate]).[2−4] The P-cluster is bound at the α/β-subunit interface by six cysteine residues, three from each subunit;[5] whereas the FeMoco resides in the α-subunit of MoFe protein.[6] During catalysis, the Fe protein and the MoFe protein undergo repeated association/dissociation cycles, where electrons are transferred from the former to the latter concomitant with ATP hydrolysis, and substrate reduction eventually takes place at the active FeMoco site upon accumulation of a sufficient amount of electrons.
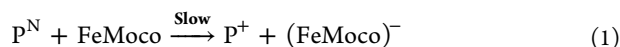
The P-cluster is believed to mediate the transfer of electrons from the [Fe$_4$S$_4$] cluster of the Fe protein to the FeMoco of the MoFe protein during nitrogenase catalysis.[1] In the resting state, the P-cluster exists in an all-ferrous form (P^N).[7] It can also exist in three other stable, oxidized states (P$^+$, P^{2+}, and P^{3+}).[8]

Formation of the P-cluster was investigated through the characterization of a so-called Δ*nifH* MoFe protein.[9] Expressed in a genetic background where the *nifH* gene (encoding the Fe protein) is deleted, the Δ*nifH* MoFe protein contains two pairs of [Fe$_4$S$_4$]-like clusters, one at each α/β-subunit interface that is normally occupied by the [Fe$_8$S$_7$] P-cluster. These [Fe$_4$S$_4$]-like cluster pairs can be reductively coupled into two mature P-clusters in a reaction involving the Fe protein and MgATP, suggesting that they are indeed the precursors to P-clusters.[9]

Two questions have arisen regarding the structural−functional relationship of the P-cluster: (1) what is the mechanistic role of the P-cluster in electron transfer from the Fe protein to the MoFe protein, and (2) why does the P-cluster possess an [Fe$_8$S$_7$] structure rather than the more common [Fe$_4$S$_4$] structure that is sufficient for electron transfer in most enzymes? The first question was tackled by a recent study,[10] which suggested a slow one-electron electron transfer from the all-ferrous P-cluster (P^N) to FeMoco (eq 1), followed by a fast reduction of the one-equivalent-oxidized P-cluster (P$^+$) by the reduced Fe protein (FeP$_{red}$) upon binding to the MoFe protein (eq 2).

$$P^N + FeMoco \xrightarrow{\text{Slow}} P^+ + (FeMoco)^- \qquad (1)$$

$$FeP_{red} + P^+ \xrightarrow{\text{Fast}} FeP_{ox} + P^N \qquad (2)$$

The P^+-state of P-cluster is obviously an important intermediate in this mechanism. However, unlike the resting (P^N, $S = 0$) and two-equivalent-oxidized (P^{2+}, $S = 3$ or 4) states of P-cluster, where various spectroscopic,[11] crystallographic,[5] and theoretical[12] studies have been undertaken, little is known of the P^+ state other than its EPR features.[13] Here, we present a variable-temperature, variable-field (VTVH) magnetic circular dichroism (MCD) spectroscopic study of the P^+ state of nitrogenase P-cluster.

2. EXPERIMENTAL SECTION

General Considerations. Unless noted otherwise, all chemicals and reagents were obtained from Fisher Scientific or Sigma-Aldrich.

Cell Growth and Purification. Wild-type (AvOP) and mutant (DJ1193)[14] strains of *Azotobacter vinelandii* were grown in 180 L batches in a 200 L New Brunswick fermentor (New Brunswick Scientific, Edison, NJ, USA) in Burke's minimal medium supplemented with 2 mM ammonium acetate. The growth rate was measured by cell density at 436 nm using a Spectronic 20 Genesys (Spectronic Instruments, Westbury, NY). After the consumption of ammonia, the cells were derepressed for 3 h, followed by harvesting using a flow-through centrifugal harvester (Cepa, Lahr, Germany). The cell paste was washed with 50 mM Tris-HCl (pH 8.0). Published methods were used for the purification of wild-type Fe protein (from AvOP), wild-type MoFe protein (from AvOP), and $\Delta nifB$ β-188^{Cys} MoFe protein (from DJ1193) of *A. vinelandii*.[15]

Protein Sample Preparation. All MCD samples were prepared in an Ar-filled drybox (Vacuum Atmospheres, Hawthorne, CA) at an oxygen level of less than 4 ppm.[16] Dithionite-reduced protein samples were in 25 mM Tris-HCl (pH 8.0), 10% glycerol, and 2 mM dithionite ($Na_2S_2O_4$). Indigodisulfonate (IDS)-oxidized protein samples were prepared by incubating samples with IDS for 5 min, followed by removal of excess IDS by a G25 size-exclusion column. Samples were subsequently concentrated in a Centricon-50 concentrator (Amicon) in anaerobic centrifuge tubes outside the drybox as described earlier.[17] After concentration, these protein samples [50–100 mg mL^{-1} in 25 mM Tris-HCl (pH 8.0) and 50% glycerol] were transferred to MCD sample cuvettes under anaerobic conditions and frozen in liquid nitrogen. MCD sample cells were constructed from optical-quality Spectrosil quartz (170–2200 nm, 1 mm path length, model BS-1-Q-1, Starna, model SUV R-1001 or FUV; Spectrocell, Oreland, PA). Each cuvette was cut into the appropriate dimensions to fit the sample holder (2.0 cm × 12.5 mm), resulting in a sample volume of approximately 160 μL. All samples contained 50% glycerol to ensure the formation of an optical glass upon freezing and were kept on dry ice in transit.

Spectroscopic Characterization. MCD spectra were recorded with a CD spectropolarimeter (model J-710; Jasco, MD) interfaced with a superconducting magnet (model Spectromag 400-7T; Oxford, U.K.) as previously described.[16] Sample temperatures were monitored with a thin film resistance temperature sensor (model CX1050-Cu-1-4L; Lakeshore, Westerville, OH) positioned directly (1 mm) above the sample cuvette. The linearity of the magnetic field was monitored with a calibrated Hall generator (model HGCA-3020; Lakeshore, Westerville, OH) placed directly outside the superconducting magnet.

MCD spectra were recorded at a rate of 50 nm min^{-1} from 800 to 350 nm at a resolution of 2–10 nm. Since optical glasses formed at low temperatures often generate a strain-induced background CD spectrum, the CD spectrum was recorded in a zero magnetic field to determine whether the background signal was excessive. If so, the sample was replaced by a new sample. To further eliminate interference by this signal, the corrected MCD spectrum was obtained for each sample by first recording the spectrum with the magnetic field in the normal direction and subtracting from it the spectrum with the

field in the reversed direction. All spectral intensities were quantified per $\alpha\beta$-dimer of the $\alpha_2\beta_2$-tetrameric MoFe protein and corrected for path length, sample concentration, and depolarization effects. The extent of depolarization was determined by placing a standard sample of nickel tartarate between the magnet cryostat and the detector. The CD spectrum was then recorded before and after light passed through the frozen protein sample in the magnet.

Analysis of Magnetization Data. Magnetization curves were recorded at a set wavelength and temperature, while the magnetic field was linearly varied from 0 to 6 T at a rate of 0.45 T min^{-1} with a resolution of 2 s. MCD data were analyzed using a fit/simulation program created by Neese and Solomon.[18] The program allows the calculation of best-fit saturation magnetization curves using experimental data as a basis set and is valid for any spin state, half-integer or integer, at any specified temperature.

Experimental data were analyzed by fitting the spin Hamiltonian parameters and the effective transition moment products. The effective transition moment products represent the planes of polarization that reflect the anisotropy of the g factors. Since the initial slope of the magnetization curve is dependent on the g factors, the transition polarizations relate the transition dipole to the g factor axes of a powder or randomly oriented sample. For $S > 1/2$ spin systems, the spin parameters, including the g factor (g), the axial zero-field splitting (D), and the rhombic distortion of the electronic environment (E/D), are determined based on the Hamiltonian (below), which is the expression for energy of the Zeeman interaction and the correction to the energy of the individual spin states arising from spin−orbit coupling.

$$\hat{H} = \beta B g\hat{S} + D[\hat{S}_z^2 - (1/3)\hat{S}(\hat{S} + 1) + (E/D)(\hat{S}_x^2 - \hat{S}_y^2)] \qquad (3)$$

At low temperatures (∼1.6 K), the lowest energy level is predominantly populated and dictates the behavior of the magnetization curve. As the temperature is raised, the spectral parameters of excited states become increasingly important in the profile of the magnetization curve. Best-fit simulations of the experimental data were initially performed at the lowest temperature to enable the determination of the spectral parameters. Subsequent simulations of high-temperature data facilitated the determination of the axial zero-field splitting, D. MCD spectral simulations were conducted using IgorPro (WaveMetrics, Inc.). Major peaks were first identified assuming a Gaussian shape. Peak intensities and central wavelengths were then adjusted and the baseline was corrected to minimize the error between the simulated and empirical curves.

3. RESULTS

The lack of information on the P^+ state is mainly due to the difficulty in generating significant concentrations of this state. The sequential oxidations of $P^N \rightarrow P^+$ and $P^+ \rightarrow P^{2+}$ exhibit the same midpoint potential (−309 mV) at pH 8,[19] and, because of this, there is not a particular potential that permits the enrichment of the P^+ state without the accumulation of high concentrations of P^N and P^{2+} states. To overcome this problem, a mutant strain of *Azotobacter vinelandii* (DJ1193) was employed in the current study.[14] There are two major advantages of using DJ1193 for spectroscopic studies of the P^+ state. First, DJ1193 contains a deletion of the *nifB* gene, which encodes an essential protein for the biosynthesis of FeMoco. As a result, the variant MoFe protein of DJ1193 lacks FeMoco, thus preventing the paramagnetic FeMoco ($S = 3/2$) from interfering with the MCD spectroscopic investigation of P-cluster. Second, DJ1193 contains a substitution of cysteine for serine at the β-188 position of the MoFe protein. The β-188^{Ser} residue is an important ligand in the structure of the P-cluster. Specifically, during the oxidation of P^N to P^{2+}, β-188^{Ser} becomes a ligand of an Fe atom in the P^{2+} state (Figure 1). The substitution of cysteine for serine in DJ1193 stabilizes the
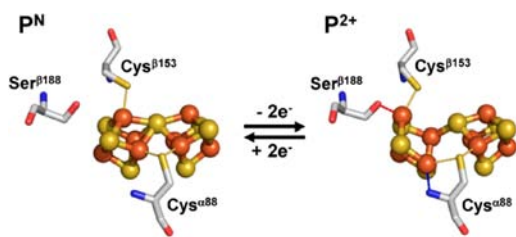
Figure 1. Structures of the P-cluster in the reduced (P^N, left) and two-equivalent oxidized (P^{2+}, right) state. The positions of residues Cys$^{\beta153}$, Ser$^{\beta188}$, and Cys$^{\alpha88}$ are shown. PYMOL was used to generate this figure using the PDB entries 3MIN and 2MIN.

Figure 3. MCD spectra of the oxidized wild-type (blue, multiplied by 1/3) and $\Delta nifB$ β-188^{cys} (red) MoFe proteins. Simulations (dashed blue and dashed red, respectively) were made using Gaussian curves (thin blue and thin red, respectively). Arrows indicate the shifts of the main transitions in the wild-type MoFe protein to those of the $\Delta nifB$ β-188^{cys} MoFe protein.

paramagnetic P$^+$ state in the as-isolated DJ1193 MoFe protein (designated the $\Delta nifB$ β-188^{Cys} MoFe protein), leading to an accumulation of 65% P-cluster in the P$^+$ state and the remaining 35% in the normal, diamagnetic P^N state.[14]

Consistent with the earlier observation that the P-cluster in the wild-type MoFe protein can be oxidized to the paramagnetic P^{2+} state, the VTVH MCD spectrum of the oxidized $\Delta nifB$ β-188^{Cys} MoFe protein (Figure 2A) exhibits decreasing
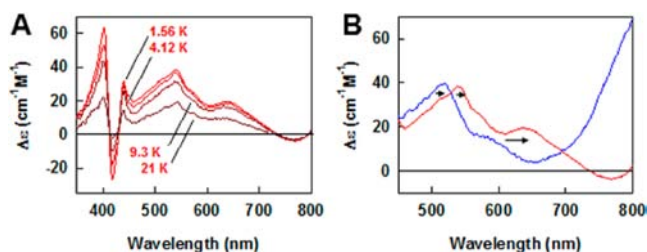

Figure 2. (A) Temperature-dependent MCD spectra of the oxidized $\Delta nifB$ β-188^{Cys} MoFe protein at 6.0 T and 1.56, 4.12, 9.3, and 21 K, respectively. Spectra were normalized for one $\alpha\beta$-dimer of the protein. Sharp inflection at 420 nm is due to a minor cytochrome impurity. (B) Comparison of the 1.6 K MCD spectra of P^{2+} in the wild-type MoFe protein (blue) and the $\Delta nifB$ β-188^{Cys} MoFe protein (red) in the high-wavelength region (450−800 nm). The spectrum of the wild-type protein was multiplied by 1/3 to allow a better visualization. Arrows represent the proposed spectral shifts of transitions in the wild-type MoFe protein relative to those in the $\Delta nifB$ β-188^{Cys} MoFe protein, as determined by the spectral simulation (see Figure 3). Concentrations of the wild-type and $\Delta nifB$ β-188^{Cys} MoFe proteins were 18.0 and 74.5 mg/mL, respectively.

spectral intensity with increasing temperature, which is indicative of a paramagnetic ground state of the P-cluster.[16] However, a closer examination of the MCD spectra of the oxidized $\Delta nifB$ β-188^{Cys} and wild-type MoFe proteins (Figure 2B) reveals both similarities and differences between them. Spectral simulations (Figure 3) of the transitions above 450 nm reveal positive bands at 486, 521, and 589 nm in the spectrum of the wild-type MoFe protein, which appear to be also present in the spectrum of the $\Delta nifB$ β-188^{Cys} MoFe protein, with bathochromic shifts to 527, 541, and 644 nm, respectively. The major difference in these spectra is the absence of a very intense, broad transition that is centered at >800 nm (simulated at 823 nm) in the spectrum of the wild-type protein. In its place, there is a broad negative transition at 740 nm in the spectrum of the oxidized $\Delta nifB$ β-188^{Cys} MoFe protein. The "823 nm" transition is the largest spectral transition in the spectrum of the oxidized wild-type protein and has been used as an identifying feature of the P^{2+} state.[16,20,21] The absence of this transition implies either a loss or a large spectral shift of a
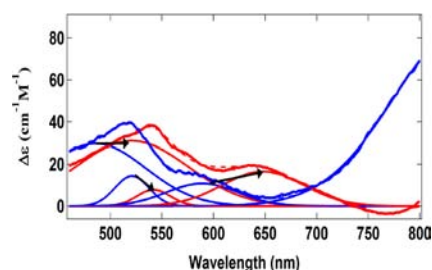
major charge-transfer transition following the substitution of cysteine for serine at the β-188 position of MoFe protein.

EPR, MCD, and Mössbauer data[8,21,22] suggest that the P^{2+} state in the wild-type MoFe protein is an $S = 3$ or 4 integer spin state. The 1.6 K magnetization curve of the oxidized $\Delta nifB$ β-188^{Cys} MoFe protein mimics that of the wild-type MoFe protein (Figure 4) in that it also exhibits a sharp initial slope,
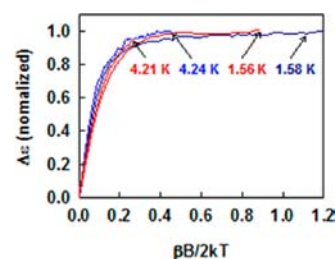

Figure 4. Comparison of the magnetization curves of the wild-type MoFe protein (blue) and the $\Delta nifB$ β-188^{Cys} MoFe protein (red) at 1.6 and 4.2 K. Data for both proteins were recorded at 770 nm.

suggesting that the P-cluster of this variant MoFe protein is present in a similar high spin state.[20,21] Such similarities between both the MCD spectra and the magnetization curves of the two MoFe proteins imply that the P^{2+} state of the $\Delta nifB$ β-188^{Cys} MoFe protein is essentially the same as that of the wild-type protein and suggest a great deal of resemblance between the electronic states of their P^{2+}-clusters.

While the MCD spectrum of the P^{2+} state reveals interesting electronic properties of this cluster, the MCD spectrum of the P$^+$ state is more pertinent to the enzymatic mechanism of nitrogenase (eq 1). The EPR spectrum of the P$^+$-cluster in the as-isolated $\Delta nifB$ β-188^{Cys} MoFe protein is virtually identical to that of the P$^+$-cluster in the wild-type MoFe protein (Table 1), showing the same mixed $S = 1/2$, $(2\times)5/2$ states that are indicative of a nearly identical electronic structure of their P-cluster species.[13,14] Consistent with this observation, the VTVH MCD spectrum of the P$^+$-cluster in the $\Delta nifB$ β-188^{Cys} MoFe protein (Figure 5A) clearly illustrates that it is present in a paramagnetic ground state. Moreover, magnetization curves of the $\Delta nifB$ β-188^{Cys} MoFe protein exhibit nesting (a fanning of the curves with temperature), implying the presence of a high-spin state component ($S > 1/2$) in this protein (Figure 5B). These curves are best simulated using a mixed paramagnetic ground state ($S = 1/2$, 5/2) with average spectral parameters obtained from the EPR spectrum of the P$^+$ state (Figure 4B).

Table 1. EPR Parameters of P⁺

MoFe protein	S	g_x[a]	g_y[a]	g_z[a]	D (cm⁻¹)	E/D	%
wild-type	1/2	2.06	1.95	1.81			11
	5/2[b]	6.7	5.3		−3.2	0.029	42
	5/2	7.3			−3.2	0.059	47
$\Delta nif B\ \beta$-188^{Cys}	1/2	2.03	1.97	1.93			55
	5/2	6.7	5.3		−3.2	0.029	20
	5/2	7.7			−3.2	0.061	25

[a]Only observed g-factors are listed. [b]Two different S = 5/2 signals are observed.
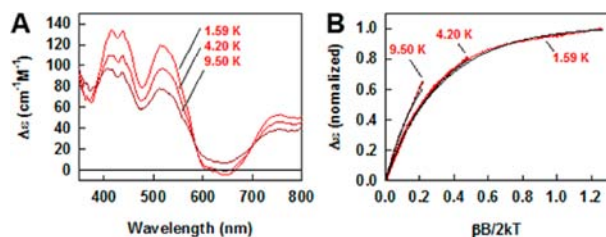

Figure 5. (A) Temperature-dependent MCD spectra of the reduced $\Delta nif B\ \beta$-188^{Cys} MoFe protein at 1.59, 4.2, and 9.5 K. Spectra were normalized for one $\alpha\beta$-dimer of the protein. (B) Magnetization curves of the reduced $\Delta nif B\ \beta$-188^{Cys} MoFe protein (red) recorded at 520 nm. Simulation of the magnetization curves (black) assuming two different spin (1/2 and 5/2) contributions and using the following parameters: 60% S = 1/2, 40% S = 5/2; for S = 5/2, D = −3 cm⁻¹, E/D = 0.003; for all curves: transition polarizations = 1.0 for the x, y, and z directions (i.e., equal contributions from all three principle axes). Protein concentration was 30.5 mg/mL.

4. DISCUSSION

It has recently been suggested that the P⁺ state of the P-cluster is a key player in the enzymatic mechanism of nitrogenase. While structures have been assigned to the P^N and P^{2+} states, the structure of P⁺ is unknown, although it has been suggested[23] to be midway between those of P^N and P^{2+}. The similarities of the MCD spectra and magnetization curves (Figures 2 and 4) of P^{2+} in the wild-type protein and the $\Delta nif B$ β-188^{Cys} MoFe protein suggest a similarity between the electronic structures of P^{2+} in both proteins. Likewise, the great similarities in the EPR parameters of P⁺ in both proteins (Table 1) suggest that the structure of the P⁺ state is also conserved in both proteins.

Most surprisingly, the MCD spectrum of the P⁺ state arises from a classic $[Fe_4S_4]^+$-like cluster.[24,25] MCD spectra have long been used to characterize the structure and redox state of basic FeS clusters.[26,27] The spectrum of a $[Fe_4S_4]^+$-like cluster exhibits a broad, derivative-like inflection that is centered around 600 nm, as well as a positive peak at ca. 520 nm and a negative trough at ca. 640 nm. Also, there is often a smaller positive peak at ca. 740 nm. Figure 5 exemplifies that these "fingerprints", which are characteristic of a $[Fe_4S_4]^+$-like cluster, are present in the MCD spectrum of the P⁺ state. This observation suggests that the wave function for the unpaired electron is localized on one 4Fe half of the P-cluster rather than delocalized over the entire 8Fe cluster. As such, it may be more correct to view the P-cluster as two linked $[Fe_4S_4]$ clusters, where each 4Fe half retains the electronic characteristic of an isolated $[Fe_4S_4]$ cluster. The suggestion of linked $[Fe_4S_4]$ clusters was previously made to explain the intensity variation

of the EPR spectrum during the stepwise oxidation of the P-cluster.[13,28] Similarly, theoretical calculations[12] have employed a split $[Fe_4S_4]$ cluster model to explain the spin state of the P^{2+}-cluster. Furthermore, the split cluster model is consistent with the identical midpoint potentials of the P$^N \rightarrow$ P⁺ and P⁺ $\rightarrow$ P^{2+} oxidations.[19] Finally, it has been shown[29] that replacing the two cysteine ligands that bridge one 4Fe half of the P-cluster with the other retains good, albeit diminished catalytic activity. It is also interesting to note that the MCD spectrum of the P⁺-cluster in the $\Delta nif B$ β-188^{Cys} MoFe protein is very similar to that of the two different $[Fe_4S_4]^+$-like clusters in the P-cluster precursor of the $\Delta nif H$ MoFe protein (Figure 6).[16,30] Such a similarity again leads to the question of why the $[Fe_8S_7]$ P-cluster is used in place of the more common $[Fe_4S_4]$ cluster for electron transfer in nitrogenase.
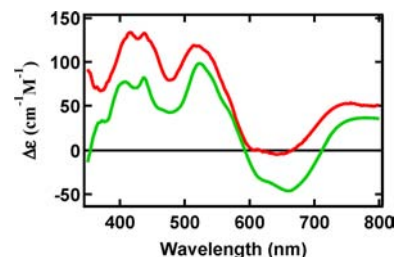

Figure 6. Comparison of the MCD spectra of P⁺ in the reduced $\Delta nif B$ β-188^{Cys} MoFe protein (red) and the $[Fe_4S_4]$-type clusters in the reduced $\Delta nif H$ (green) MoFe proteins at a temperature of 1.6 K and a magnetic field of 6.0 T. Spectra were normalized for one $\alpha\beta$-dimer of the protein. The intensity of the $\Delta nif H$ MoFe protein spectrum was multiplied by 0.5 to compensate for the presence of two $[Fe_4S_4]$-type clusters in the protein, compared with the presence of a single P-cluster in the $\Delta nif B$ β-188^{Cys} MoFe protein. The positive shift of the spectrum of $\Delta nif B$ β-188^{Cys} MoFe protein relative to that of the $\Delta nif H$ MoFe protein is likely caused by the presence of an S = 5/2 spin state in the former protein.

The answer to this question may be drawn indirectly from studies of proteins similar to the MoFe protein. DPOR (dark operative protochlorophillide reductase) and COR (chlorophyllide a reductase), two enzymes involved in bacteriochlorophyll synthesis,[31,32] are good examples of these MoFe protein homologues. Both DPOR and COR contain only a single $[Fe_4S_4]$ cluster in an analogous position held by the P-cluster in the MoFe protein, and both are capable of catalyzing two-electron reduction of substrates: DPOR catalyzes the two-electron reduction of the D-ring of porphoryrin, and COR catalyzes the subsequent two-electron reduction of the B-ring of chlorin.[31,32] Similarly, NifEN, another functional homologue to the MoFe protein, contains a single $[Fe_4S_4]$ cluster at a position that corresponds to the position of P-cluster in the MoFe protein.[33] Like DPOR and COR, NifEN can catalyze the two-electron reduction of certain substrates (i.e., C_2H_2 and N_3^-), but it cannot reduce these substrates further, nor can it reduce other nitrogenase substrates that require more electrons (e.g., CN⁻, N_2H_4, and N_2).[34]

The fact that all these MoFe protein homologues can only catalyze two-electron reduction via their respective $[Fe_4S_4]$ cluster suggests that the more complex $[Fe_8S_7]$ P-cluster is required specifically for the reduction of substrates that involve the transfer of more than two electrons, such as N_2. The Lowe–Thorneley (LT) model of N_2 reduction[30] involves eight one-electron transfer steps from the Fe protein to the MoFe

protein (Figure 7), with E_0 representing the enzyme in the resting state and E_n representing the enzyme after receiving n
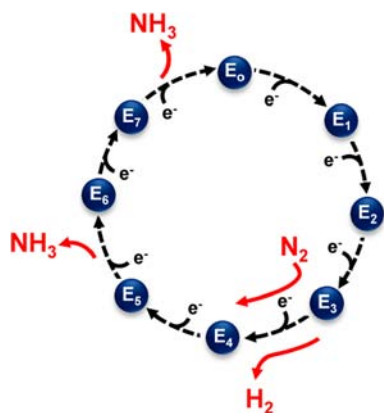

Figure 7. Lowe−Thorneley (LT) model for N_2 reduction by nitrogenase. The resting state of one-half of the MoFe protein is represented by E_0. State E_n represents the protein after having received n electrons from the Fe protein and n protons from the medium. The LT model proposes that the binding of N_2 occurs at the E_3 or E_4 step and the release of NH_3 occurs at E_5 or E_7 step.

electrons and n protons (where $8 \geq n \geq 0$). The "electron inventory"[35] states that the n electrons are associated with the number transferred to the cofactor (m) and the substrate (s) and the number oxidized at the P-cluster (p), such that $n = m + s − p$. Data obtained from previous studies suggest that the initial binding of N_2 occurs at the E_3 or E_4 step and the reduction of N_2 occurs at higher E_n steps.[36]

A basic premise of the LT model is that each step involves the transfer of only one electron. This premise is centered on two assumptions. The first assumption is that the Fe protein can transfer only one electron to the MoFe protein during each step in the cycle (Figure 7). While it has been shown[37] that the FeS cluster in the Fe protein can be super-reduced to the all ferrous $[Fe_4S_4]^0$ state, thus making it a potential two-electron donor, there is no definitive proof that such a two-electron transfer process indeed occurs during enzymatic turnover. The second assumption is that the Fe protein first reduces the P-cluster, which subsequently reduces the FeMo cofactor. The recent proposal[10] (eqs 1 and 2) seems to be just the opposite of this assumption, and if the P-cluster indeed donates an electron to FeMoco first (eq 1), then there is no longer a restriction on a strict one-electron transfer in this process.

The results presented herein suggest that the P-cluster may act as two coupled $[Fe_4S_4]$ clusters, each capable of donating one electron to FeMoco. In this case, the P-cluster could undergo either a one- or two-electron transfer process as a complete unit. Over the past few decades, a vast amount of research has gone into the study of the mechanism and kinetics of nitrogenase. By far the majority of these studies focused on the early steps of the LT cycle, where the concept of one-electron transfer per step is favored.[1] Our hypothesis is consistent with this concept and the earlier proposal that the initial $E_0 \rightarrow E_1$ mechanistic step involves one electron (eq 1). However, it can also be used to further reason that one or more of the steps later in the LT cycle may involve two electrons, followed by reduction of P^{2+} back to P^N.

In an intra-MoFe protein two-electron transfer, $n = 0$ and $p = 2$, meaning $m + s = 2$. Recent spectroscopic data[38] suggests that the cofactor only cycles through two different states, the native

state (M^N) and the one-electron reduced state (M^R). As such, a two-electron transfer would likely leave m unchanged resulting in both electrons residing on the substrate ($s = 2$). Since the two-electron transfer event is suggested to occur later in the cycle, on which few, if any, experiments have focused, there is currently no evidence to either support or refute this theory. Regardless, there could be an energy advantage to the two-electron transfer event. Calculations[39,40] show that the major energy barriers to N_2 reduction occur during the initial "uphill" reduction steps. The mechanistic step in the two-electron transfer process may be required to more efficiently surmount the energy barriers of this reaction. Given the two 4Fe halves in the 8Fe structure of P-cluster, it is possible that the MoFe protein utilizes two different electron transfer pathways from the P cluster to FeMoco, each originating from a different half of the P cluster.

There could also be a kinetic advantage to the two-electron transfer process. One of the side reactions (eq 3) in the LT model[35] is the slow, natural relaxation of E_n state to lower ($E_{n−2}$) states with the concomitant evolution of H_2.

$$E_n + 2H^+ \xrightarrow{\text{Slow}} E_{n−2} + H_2 \qquad (3)$$
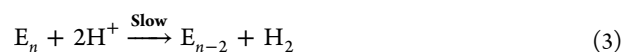
It is obvious that this reaction decreases the ability of the enzyme to reach higher E_n state and, consequently, lowers the efficiency of the nitrogenase reaction. However, the two-electron transfer mechanism could counteract this inefficient side reaction by more rapidly "pushing" the enzyme to higher E_n states that are necessary for the binding and reduction of N_2.

In summary, the MCD spectrum of the P^+-cluster in $\Delta nifB$ β-188^{Cys} MoFe protein has been identified as arising from a $[Fe_4S_4]^+$-like cluster, suggesting that the P-cluster may function as two coupled $[Fe_4S_4]$-like clusters, where each cluster is capable of transferring electrons to FeMoco. Such a cluster arrangement of P-cluster is likely related to the mechanism of N_2 reduction and could serve as a focal point of future investigations of the structure−function relationship of nitrogenase.

■ AUTHOR INFORMATION

Corresponding Author
mribbe@uci.edu; bhales@lsu.edu

Author Contributions
The manuscript was written through contributions of all authors. All authors have given approval to the final version of the manuscript.

Notes
The authors declare no competing financial interest.

■ REFERENCES

(1) Burgess, B. K.; Lowe, D. J. *Chem. Rev.* **1996**, *96*, 2983−3011.
(2) Chan, M. K.; Kim, J.; Rees, D. C. *Science* **1993**, *260*, 792−794.
(3) Spatzal, T.; Aksoyoglu, M.; Zhand, L.; Andrade, S. L. A.; Schleicher, E.; Weber, S.; Rees, D. C.; Einsle, O. *Science* **2011**, *334*, 940.
(4) Lancaster, K. M.; Roemelt, M.; Ettenhuber, P.; Hu, Y.; Ribbe, M. W.; Neese, F.; Bergmann, U.; DeBeer, S. *Science* **2011**, *334*, 974−977.
(5) Einsle, O.; Tezca, F. A.; Andrade, S. L. A.; Schmid, B.; Yoshida, M.; Howard, J. B.; Rees, D. C. *Science* **2002**, *297*, 1696−1700.
(6) Peters, J. W.; Stowell, M. H. B.; Soltis, S. M.; Finnegan, M. G.; Johnson, M. K.; Rees, D. C. *Biochemistry* **1997**, *36*, 1181−1187.

(7) Münck, E.; Rhodes, H.; Orme-Johnson, W. H.; Davis, L. C.; Brill, W. J.; Shah, V. K. *Biochim. Biophys. Acta* **1975**, *400*, 32−53.

(8) Pierik, A., J.; Wassink, H.; Haaker, H.; Hagen, W. R. *Eur. J. Biochem.* **1993**, *212*, 51−61.

(9) Hu, Y.; Fay, A. W.; Lee, C. C.; Ribbe, M. W. *Proc. Natl. Acad. Sci. U.S.A.* **2007**, *104*, 10424−10429.

(10) Danyal, K.; Dean, D. R.; Hoffman, B. M.; Seefeldt, L. C. *Biochemistry* **2011**, *50*, 9255−9263.

(11) Dunham, W. R.; Hagen, W. R.; Braaksma, A.; Haaker, H.; Gheller, S.; Newton, W. E.; Smith, B. In *Nitrogen Fixation; Research Progress*; Evans, H. J., Bottomley, P. J., Newton, W. E., Eds.; Martinus Nijhoff: Dordrecht, Boston, Lanchaster, 1985; pp 591−596.

(12) Noodleman, L.; Lovell, T.; Liu, T.; Himo, F.; Torres, R. A. *Curr. Opin. Chem. Biol.* **2002**, *6*, 259−273.

(13) Tittsworth, R. C.; Hales, B. J. *J. Am. Chem. Soc.* **1993**, *115*, 9763−9767.

(14) Chan, J. M.; Christiansen, J.; Dean, D. R.; Seefeldt, L. C. *Biochemistry* **1999**, *38*, 5779−5785.

(15) Burgess, B. K.; Jacobs, D. B.; Stiefel, E. I. *Biochim. Biophys. Acta* **1980**, *614*, 196−209.

(16) Broach, R. B.; Rupnik, K.; Hu, Y.; Fay, A. W.; Cotton, M.; Ribbe, M. W.; Hales, B. J. *Biochemistry* **2006**, *45*, 15039−15048.

(17) Bursey, E. H.; Burgess, B. K. *J. Biol. Chem.* **1998**, *273*, 29678−29685.

(18) Neese, F.; Solomon, E. I. *Inorg. Chem.* **1999**, *38*, 1847−1865.

(19) Lanzilotta, W. N.; Christiansen, J.; Dean, D. R.; Seefeldt, L. C. *Biochemistry* **1998**, *37*, 11376−11384.

(20) Johnson, M. K.; Thomson, A. J.; Robinson, A. E.; Smith, B. E. *Biochim. Biophys. Acta* **1981**, *671*, 61−70.

(21) Morningstar, J. E.; Johnson, M. K.; Case, E. E.; Hales, B. J. *Biochemistry* **1987**, *26*, 1795−1800.

(22) Surerus, K. K.; Hendrich, M. P.; Christie, P. D.; Rottgardt, D.; Orme-Johnson, W. H.; Münck, E. *J. Am. Chem. Soc.* **1992**, *114*, 8579−8590.

(23) Mayer, S. M.; Lawson, D. M.; Gormal, C. A.; Roe, S. M.; Smith, B. E. *J. Mol. Biol.* **1999**, *292*, 871−891.

(24) Conover, R. C.; Kowal, A. T.; Fu, W.; Park, J.-B.; Aono, S.; Adams, M. W. W.; Johnson, M. K. *J. Biol. Chem.* **1990**, *265*, 8533−8541.

(25) Onate, Y. A.; Finnegan, M. G.; Hales, B. J.; Johnson, M. K. *Biochim. Biophys. Acta* **1993**, *1164*, 113−123.

(26) Johnson, M. K.; Thomson, A. J.; Robinson, A. E.; Rao, K. K.; Hall, D. O. *Biochim. Biophys. Acta* **1981**, *667*, 433−451.

(27) Johnson, M. K.; Robinson, A. E.; Thomson, A. J. In *Iron-Sulfur Proteins*; Spiro, T. G., Ed.; Wiley-Interscience: New York, 1982; pp 367−406.

(28) Tittsworth, R. C.; Hales, B. J. *Biochemistry* **1996**, *35*, 479−489.

(29) Yousafai, F. K.; Buck, M.; Smith, B. E. *Biochem. J.* **1996**, *318*, 111−118.

(30) Rupnik, K.; Lee, C. C.; Hu, Y.; Ribbe, M. W.; Hales, B. J. *J. Am. Chem. Soc.* **2011**, *133*, 6871−6873.

(31) Nomata, J.; Mizoguchi, T.; Tamiaki, H.; Fujita, Y. *J. Biol. Chem.* **2006**, *281*, 15021−15028.

(32) Watzlich, D.; Brocker, M. J.; Uliczka, F.; Ribbe, M. W.; Virus, S.; Jahn, D.; Mose, J. *J. Biol. Chem.* **2009**, *284*, 15530−15540.

(33) Kaiser, J. T.; Hu, Y.; Wiig, J. A.; Rees, D. C.; Ribbe, M. W. *Science* **2011**, *331*, 91−94.

(34) Hu, Y.; Yoshizawa, J.; Fay, A. W.; Lee, C. C.; Wiig, J. A.; Ribbe, M. W. *Proc. Natl. Acad. Sci. U.S.A.* **2009**, *106*, 16962−16966.

(35) Lee, H. I.; Sørlie, M.; Christiansen, J.; Yang, T. C.; Shao, J.; Dean, D. R.; Hales, B. J.; Hoffman, B. M. *J. Am. Chem. Soc.* **2005**, *127*, 15880−15890.

(36) Thorneley, R. N. F.; Lowe, D. J. In *Molybdenum Enzymes*; Spiro, T. G., Ed.; John Wiley & Sons: New York, 1985; Vol. 7, pp 221−284.

(37) Watt, G. D.; Reddy, K. R. N. *J. Inorg. Biochem.* **1994**, *53*, 281−294.

(38) Doan, P. E.; Telser, J.; Barney, B. M.; Igarashi, R. Y.; Dean, D. R.; Seefeldt, L. C.; Hoffman, B. M. *J. Am. Chem. Soc.* **2011**, *133*, 17329−17340.

(39) Igarashi, R. Y.; Seefedt, L. C. In *Catalysts for Nitrogen Fixation*; Smith, B. E., Richards, R. L., Newton, W. E., Eds.; Kluwer Academic Publishers: Dorddrecht/Boston/London, 2004; pp 97−140.

(40) Kurnikov, I. V.; Charnley, A. K.; Beratan, D. N. *J. Phys. Chem. B* **2001**, *105*, 5359−5367.